

## MAMMALIAN SPINAL BIOMECHANICS

### I. STATIC AND DYNAMIC MECHANICAL PROPERTIES OF INTACT INTERVERTEBRAL JOINTS

BY JULIANNA M. GÁL\*

Department of Pure and Applied Biology, University of Leeds, Leeds, LS2 9JT, UK

Accepted 24 August 1992

#### Summary

Four-point bending was used to apply pure extension and flexion moments to the ligamentous lumbosacral spine and pelvic girdle of monkey (*Macaca fascicularis*), rabbit (domestic and wild, *Oryctolagus cuniculus*), badger (*Meles meles*), wallaby (*Wallabia rufogrisea fruticosa*), sheep (*Ovis aries*), seal (*Phoca vitulina*) and tiger (*Panthera tigris*). The absolute ranges of angular change in lumbar–lumbar joints (from X-radiographs) were considerable and similar in monkey and wallaby (greater in flexion) and in rabbit and badger (symmetrical in extension and flexion). Mass-specific bending comparisons showed that monkey and seal joints were the most and least resistant, respectively, to these moments. The patterns of mobility showed no clear scaling effects. Subsequently, additional ligamentous joint complexes (three vertebrae and two intervertebral discs) of monkey, wallaby, tiger, jaguar (*Panthera onca*) and seal (*Halichoerus grypus*) were subjected to cyclic extension and flexion moments. Changes in intervertebral angle ( $y$ , from X-radiographs) were modelled as functions of applied specific bending moments ( $x$ ):  $y=A(1-e^{-Bx})$ .  $A$  and  $B$  values represented bending capacities and joint compliances respectively. Homologous monkey and wallaby joints had considerable flexion capacities, with low compliances. Homologous jaguar and tiger joints had limited flexion capacities, but greater compliances. The data suggest that flexion resistance may be controlled by different mechanisms in different species.

#### Introduction

‘Standing four-square upon its fore-legs and hind-legs, with the weight of the body suspended between, the quadruped at once suggests to us the analogy of a bridge, carried by its two piers.’

This statement, extracted from D’Arcy Thompson’s (1917) treatise, *On Growth and Form*, typifies early considerations of the functional morphology of the quadrupedal (particularly mammalian) vertebral column. With the emphasis upon the supporting role

\*Present address: Human Performance Laboratory, Faculty of Physical Education, University of Calgary, 2500 University Drive NW, Calgary, Alberta, Canada T2N 1N4.

Key words: mammals, intervertebral joints, bending, strain energy, compliance, resilience.

of the column, the merits of several bridge and bow-and-string analogies have been discussed (Thompson, 1917; Rockwell *et al.* 1938; Slijper, 1946; Badoux, 1968, for example). These early authors were primarily concerned with the overall performance of the tetrapod vertebral column as a static supporting member. Anatomical features were mentioned and discussed, but the qualitative observations were rarely supported with experimentation or even measurements. More recently, attempts were made to correlate bending resistance with intervertebral joint morphology. The near-circular cross sections of the vertebral centra were thought to maximize bending resistance. The articular joints strengthened the column and interlocking processes further restricted movement (Jeffcott and Dalin, 1980; Townsend *et al.* 1983; Townsend and Leach, 1984; Halpert *et al.* 1987, for example). In all of these studies, joint movement was viewed rather negatively, as something to be controlled and restricted. While man-made support structures (e.g. bridges) are very often specifically designed to exclude any movement, controlled mobility, at least to some degree, is essential in the vertebral column of the living animal.

Others have focused on the importance of spinal mobility. Hildebrand (1959) suggested that the sprinting performance of the cheetah was related to the pronounced extension and flexion of the lumbosacral column. Ground contact time and stride length would be increased by enhanced sagittal spinal mobility. Similarly, Hurov (1987) concluded that bending the back significantly enhanced galloping performance in the vervet monkey. Alexander *et al.* (1985) argued that the recruitment of dorsal musculature also involved the recruitment of a dorsal spring system. They suggested that the kinetic energy associated with limb swing could be stored briefly as elastic strain energy primarily in the stretched aponeurosis of the longissimus dorsi muscle of the flexed back. Subsequent spinal extension and recoil of the aponeurosis would restore some of the kinetic energy required to reaccelerate the limbs in the opposite direction. In this way, spinal mobility could have a direct effect on the energetics of locomotion. Indeed, Alexander (1988) suggested that mammals switch from a trot to a gallop because recruitment of this spring system made galloping the most economical gait for higher speeds.

The link between vertebral morphology, column support and energetics was investigated extensively by Smeathers (1981). He observed that many smaller animals tended to have long arched flexible lumbar columns, while larger animals tended to possess short straight stiffer lumbar columns. He suggested that the differences in morphology were related to the metabolic cost of maintaining column stability. The small mammal lumbar morphology permitted a wide range of spinal curvatures with a minimum resistance. In adopting a vertebral column that facilitated rapid movements, muscular effort, and therefore metabolic energy, would be required to maintain posture. In contrast, he argued that large mammals with stiff straight backs had intrinsically stable columns. Maintenance of posture in these animals was largely passive. The loss of mobility was compensated by saving metabolic energy associated with active muscular stability. Large less-active mammals were thought to benefit from this type of column. He cited large grazing bovids as examples to illustrate this idea.

Variations in the orientation and morphology of the mammalian vertebral column are striking. Despite this, Smeathers' (1981) study remains one of very few involving non-

human mammalian vertebral mechanics, particularly from an experimental perspective. He used Euler buckling theory to measure the sagittal and lateral bending stiffness of goat and rabbit lumbar spines (stiff-back and flexible-back lumbar morphologies respectively). He also performed mechanical tests with isolated intervertebral components and determined which structures were most important in exerting bending resistances. Alexander *et al.* (1985) tested the vertebral centra and intervertebral discs of dog and deer under axial compression, and calculated their capacity for the storage and release of elastic strain energy.

In contrast, the static and dynamic load-deformation behaviour of the human vertebral column and intervertebral joints thereof continues to be the subject of intense investigation. Mechanical responses to axial compression, lateral and sagittal bending, lateral and sagittal shear, axial torsion and combinations thereof have been investigated (Jayson, 1980; Hansson *et al.* 1986; Miller *et al.* 1986; Edwards *et al.* 1987; Shirazi-Adl and Drouin, 1987; Smeathers and Joanes, 1988; Yamamoto *et al.* 1989; Yoganandan *et al.* 1989; Kim and Goel, 1990; Osvalder *et al.* 1990; and White and Panjabi, 1990, for example). By making detailed measurements of the load-deformation responses of axial components in isolation and in intact spinal motion segments (for example), researchers endeavour to understand the methods by which external loads are supported by the column in normal healthy individuals and in those afflicted by the myriad of vertebral pathologies. The ability to predict the mechanical behaviour of the spine under normal and diseased conditions has obvious implications for public health and awareness and, more specifically, for the treatment and prevention of spinal dysfunction.

Smeathers argued that the loss of mobility incurred by large stiff-backed mammals was compensated by the passive maintenance of posture. However, these animals, like the horse and large bovids for example, are not totally lacking in vertebral mobility. Rather, it tends to be almost exclusively isolated in the lumbosacral joint (Jeffcott and Dalin, 1980; Townsend *et al.* 1983; Townsend and Leach, 1984; Halpert *et al.* 1987, for example). Perhaps it was not so much about the presence or absence of vertebral column mobility, but more a question of distribution of mobility among the intervertebral joints within the column. A joint-by-joint assessment of intervertebral mobility for a wide variety of mammalian species seemed to be a useful starting point for a series of studies aimed at a better understanding of mammalian vertebral functional morphology.

This series of studies began with an exploratory investigation of passive intervertebral mobility of the lumbosacral column and pelvic girdle of a wide variety of mammalian species: monkey (*Macaca fascicularis*), rabbit (*Oryctolagus cuniculus*), wallaby (*Wallabia rufogrisea fruticosa*), badger (*Meles meles*), sheep (*Ovis aries*), seal (*Phoca vitulina*) and tiger (*Panthera tigris*). Four-point bending was used to apply uniform extension and flexion moments to all lumbar–lumbar, lumbosacral and iliosacral joints, and intervertebral angles were measured. Geometric, elastic and static stress similarity theories (McMahon, 1973, 1975) were used to determine whether sagittal bending responses show any scaling effects.

The fact that intervertebral joints are also subject to dynamic loading had to be acknowledged. Therefore, on the basis of bending asymmetries observed in the static bending tests, a subset of the original group of species was chosen for the subsequent

cyclic bending experiments. Additional lumbar–lumbar and lumbosacral specimens from monkey, wallaby, tiger, jaguar (*Panthera onca*) and seal (*Halichoerus grypus*) were sectioned into intervertebral joint complexes and subjected to dynamic three-point bending tests. Measurements of specific dynamic bending moments, changes in intervertebral angle and the specific strain energies absorbed in deformation were made. Mathematical models were used to quantify bending ranges and resistances for each lumbar joint of each species. Differences between the parameters of the specific bending and strain energy absorption models suggest that although extension behaviour was similar for the terrestrial species, flexion behaviour appeared to be governed by different mechanisms in each species.

### **Materials and methods**

#### *The static bending experiments*

##### *Animals and specimen preparation*

The species used for the static bending experiments were monkey (*Macaca fascicularis*), rabbit (domestic and wild, *Oryctolagus cuniculus*), badger (*Meles meles*), wallaby (*Wallabia rufogrisea fruticosa*), sheep (*Ovis aries*), seal (*Phoca vitulina*) and tiger (*Panthera tigris*) (Burton, 1972; Burton and Burton, 1979; Burn, 1980). They were derived from a variety of sources. The wallabies (three individuals) and tiger (one only) came from Whipsnade Zoo, as part of their population control program. They were either sent directly to the biology department, or were dissected on site at the zoo and then transported. In either case, they were used directly or frozen immediately for future use, within 24h of death. The monkeys (three individuals) were sent fresh from a primate research laboratory to the department and were frozen upon arrival. The domestic rabbits (three individuals) came from the Department of Biochemistry at the University of Leeds, and were frozen directly. The wild rabbits (three individuals) were obtained from A. Foster's stall at the Leeds City (Kirkgate) Market. They were Yorkshire rabbits, shot in the wild only hours before arrival at the market stall. They were obtained prior to dressing by the shopkeeper and were fresh and intact. Again, they were either used directly or frozen for future use. The badgers (two individuals) were road-kills, which were held in cold storage shortly after their demise. Subsequently, they were transported to the department and frozen. As they did not appear gamey following thaw, they were deemed suitable for experimentation. The sheep (three individuals) were obtained from the Department of Animal Physiology and Nutrition at the University of Leeds, and were frozen immediately. The seal (one only) was found on the North Sea Coast shortly after death. It was collected by Dr Caroline Pond. Following dissections for her own work, she dispatched the remaining lower lumbar, sacral and hind-flipper portion to Leeds, where it was subsequently frozen, not more than 1–2 days following death. All animals were apparently healthy prior to death except the seal, which was almost certainly a victim of the North Sea canine distemper epidemic of 1988. Although the animals derived from other departments within the university were subject to previous experimentation, they were thought to have suffered no adverse musculoskeletal effects, except perhaps through lack of exercise. Animals were stored at approximately  $-20^{\circ}\text{C}$  in walk-in freezer rooms.

The ligamentous spine and pelvic girdle was isolated from each animal by the following protocol. Each animal was skinned and the head was removed at the atlas-axis articulation. The hind limbs were removed at the hip joints. Abdominal muscles (external and internal obliques, and rectus abdominus) were removed to allow dissection of the forelimbs at the scapulae. Ribs were removed by sawing. Major axial extensors (longissimus and multifidus) and flexors (psoas major and minor) were carefully dissected off and weighed. The lumbar spine and pelvic girdle were isolated by the removal of the remaining thoracic elements, 1–4 thoracic vertebrae cranial to the first lumbar vertebra. Intervertebral muscles, ligaments and connective tissues were left intact. Specimens were kept moist at all times with distilled water, moistened paper towelling and plastic film.

#### *Apparatus and theory*

The apparatus used to apply pure extension and flexion (sagittal) bending moments to the specimens is illustrated in Fig. 1. The bending frame consisted of two wooden planks, nailed to the lateral margins of a wooden platform. The planks supported the bars on which the pulleys glided. A wooden arm was fixed to one of the lateral supports. The pelvic end of the specimen was fixed as rigidly as possible to this arm, either by string (smaller specimens) or by G-clamp (larger specimens). The thoracic end of the specimen was attached as rigidly as possible to a wooden block. Each attachment effectively furnished two points of contact, hence the 'four-point' bending. The wooden block was bolted to a circular wooden disc. The disc had six radially-oriented screw pins. Chains could be attached to opposing pins, to which weights could be secured. The chains ran over pulleys and down the sides of the bending frame. The frame was supported on a wooden box, approximately 30cm from the floor. The X-ray head was mounted about 1.3–1.5m above the frame and specimen. When the specimen was secured, weights were attached to diagonally opposite pins. The forces exerted by the weights about the pins applied a torque to the wooden disc and bent the specimen. The pulleys were subsequently adjusted to keep the chains parallel. X-rays were taken of the bent specimens. Chain height was kept as closely as possible to the height of the central long axis of the specimen to minimize axial torque.

It can be shown that, if the forces applied to the wooden disc and the attached specimen are parallel and of equal magnitude, the bending moment will be uniform along the length of the specimen (refer to Fig. 1A). Let  $A$  be a point on the central axis of the specimen. Let  $F_1$  and  $F_2$  be the forces exerted by the weights, attached to chains on opposing screws. Let  $L$  be the perpendicular distance between point  $A$  and  $F_1$ . If  $X$  is the perpendicular distance between  $F_1$  and  $F_2$ , then the bending moment at  $A$  is:

$$M_A = F_1 L - F_2 (L - X).$$

If  $F_1 = F_2 = F'$ , then:

$$M_A = F' X.$$

So, if equal weights are hung from each chain, then the moment at any point along the specimen's length will be the product of the force exerted by the weight ( $F'$ ) and the perpendicular distance between the lines of action ( $X$ ).

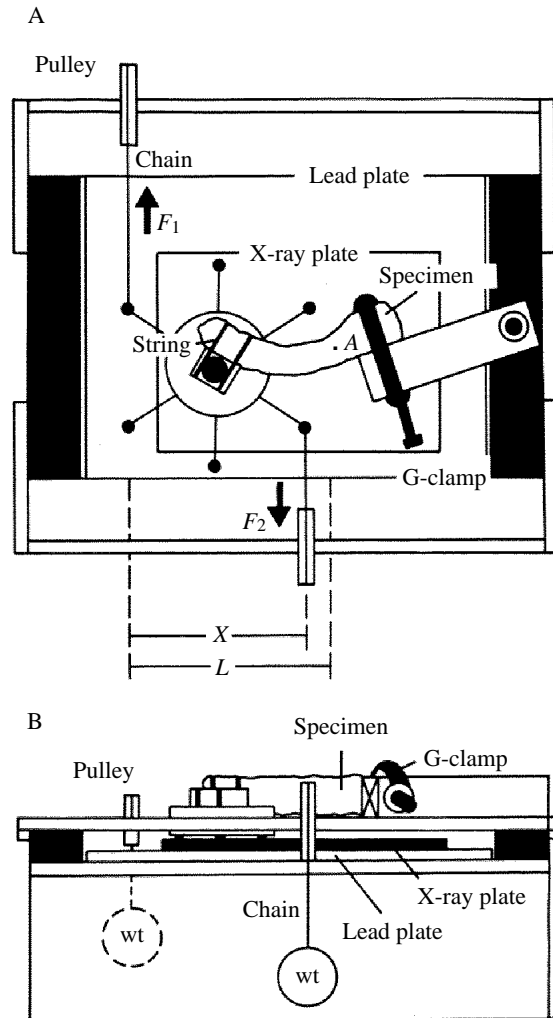


Fig. 1. The four-point bending apparatus is shown from above (A) and from the side (B). When equal weights are suspended from opposing parallel chains, the bending moment at any point along the length of the specimen will be equal to the product of the force exerted by the weight on a chain and the perpendicular distance between the parallel chains. See text for further explanation.

X-rays were taken for a series of extension (dorsal concave, positive bending) and flexion (dorsal convex, negative bending) moments. Specimens were bent in extension and flexion by alternating the direction of the chains on opposing pins. X-rays were also taken of unloaded (resting) specimens, which were lightly tapped in both the flexion and extension directions and allowed to settle to equilibrium positions before exposure. The mean differences between the extremes of the unloaded joint angles were compared using paired Student's *t*-tests (Sokal and Rohlf, 1981). The null hypothesis for each test was that the mean unloaded difference was not significantly different from zero. The null

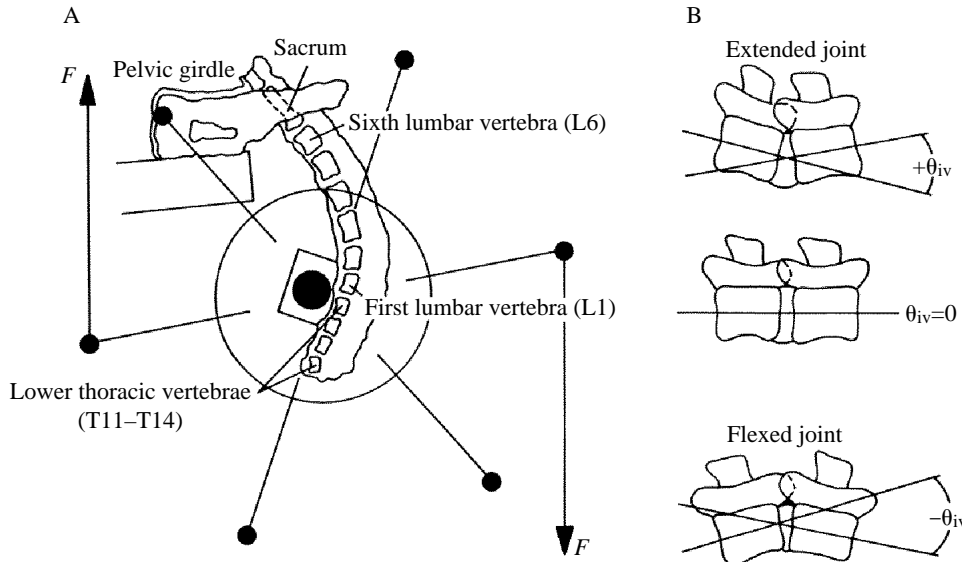


Fig. 2. An X-ray tracing of a flexed wallaby lumbosacral column is shown in A, with the directions of pull of the chains indicated. The schematic diagram (B) illustrates the methods for measuring intervertebral angle ( $\theta$ ) and assigning algebraic signs to the bent intervertebral joints. See text for further explanation.

hypothesis was rejected if the calculated  $t$ -statistic was greater than the 95% confidence  $t$ -statistic, taken from standard statistical tables (Rohlf and Sokal, 1981). A significant unloaded angular range was referred to as the neutral zone of the joint.

#### Data analyses

Tracings were made from each X-ray plate corresponding to a specific specimen and applied bending moment (see Fig. 2A). The angles of lumbar–lumbar, lumbosacral and iliosacral joints were measured by estimating the angles between the central long axes of the bones with a protractor. A convention was chosen such that angles became more positive with increased extension, and more negative with increased flexion (see Fig. 2B). A further convention was used to name the intervertebral joints. Lumbar vertebrae were numbered from the cranial (thoracic) to the caudal (sacral) end of the column (Getty, 1975). Thus, the intervertebral joint between the second and third lumbar vertebrae was called L2L3. The error associated with using this technique for measuring intervertebral angle was determined by taking ten tracings of a single random X-radiograph. Intervertebral angles were measured for each joint, and mean angles and standard errors were calculated. The average standard error was used as an indication of the measurement error.

In order to study the effects of increasing specimen size on the bending moments applied and the subsequent changes in intervertebral angle, geometric similarity theory (McMahon, 1973, 1975) was used. 'Equivalent moments' were derived as shown below (refer to Fig. 3A). Consider two vertebrae, with an intervertebral disc of thickness  $t$ .

Bending moments  $M$  are applied to this complex, bending it through an angle  $\theta$ .  $\theta$  is related to the thickness  $t$  and the radius of curvature of the bent complex  $r$ , by:

$$\theta \cong t/r \quad (1)$$

(when  $\theta$  is expressed in radians). The standard equation for bending (beams, Timoshenko and MacCullough, 1948) is:

$$M = EI/r, \quad (2)$$

where  $E$  is Young's modulus and  $I$  is the second moment of area of a cross section about the neutral axis. Rearranging equation 2, substituting it into equation 1 and solving for  $\theta$  gives:

$$\theta = Mt/EI. \quad (3)$$

For geometrically similar animals, all linear dimensions are proportional. Therefore:

$$I \propto \text{length}^4$$

$$t \propto \text{length}.$$

So:

$$I/t \propto \text{length}^3 \propto \text{volume} \propto \text{mass}$$

for animals of equal density and equation 3 can be written as:

$$\theta \propto M/E\text{mass}. \quad (4)$$

If the animals being compared are geometrically similar, and made of the same materials, then plotting intervertebral angles as functions of bending moment/body mass should yield the same results for all animals.

McMahon (1973, 1975) developed and used two additional theoretical models in an effort to reconcile the published data on skeletal dimensions in animals, with their mechanical and physiological performance during running. These were elastic similarity and static stress similarity. Elastically similar animals were deemed those whose structures were similarly threatened by elastic failure (buckling) under their own weight. McMahon showed that, for them:

$$\text{length} \propto \text{diameter}^{2/3},$$

where length and diameter referred to linear dimensions parallel and perpendicular to the long axis of the structure respectively. Applying this idea to the bending of intervertebral joints gives:

$$I \propto \text{diameter}^4.$$

and

$$t \propto \text{length}.$$

So:

$$I/t \propto \text{diameter}^{10/3} \propto \text{mass}^{5/4}$$

(because  $\text{diameter} \propto \text{weight}^{3/8}$ ). Equation 3 would now be written as:

$$\theta \propto M/E\text{mass}^{5/4}. \quad (5)$$

Therefore, for elastic similarity, plotting intervertebral angles as functions of bending moment/body mass<sup>5/4</sup> should yield the same results for all animals.

McMahon referred to static stress similarity as the alteration of linear dimensions to maintain maximum stresses in self-loading. Animals with this design criterion would have:

$$\text{length} \propto \text{diameter}^{1/2}.$$

Considering the bending joints:

$$I \propto \text{diameter}^4$$

and

$$t \propto \text{length}.$$

So:

$$I/t \propto \text{diameter}^{7/2} \propto \text{mass}^{7/5}$$

(because diameter  $\propto$  weight<sup>2/5</sup>). So, equation 3 would be written as:

$$\theta \propto M/E\text{mass}^{7/5}. \quad (6)$$

For static stress similarity, plotting intervertebral angles as functions of bending moment/body mass<sup>7/5</sup> should yield the same results for all animals. As with geometric similarity, the elastic and static stress similarity models assume animals of equal density, and ligaments and intervertebral discs etc. of equal Young's modulus.

Fig. 3B illustrates how the static bending results were analyzed and presented. Positive moments extended the joints and negative moments flexed the joints. The mean unloaded angle of each joint was calculated by considering all specimens in each species. Best-fitting curves were drawn by eye through the data set of each joint (of each species) from the mean unloaded angle. Differences from this mean to approximate plateaus in extension and flexion were defined as the forced ranges. To compare behaviour under the influence of low and high bending moments, equal positive and negative ratios of bending moment/body mass were located, and corresponding angles were taken from the hand-drawn curves.

### *The dynamic bending experiments*

#### *Animals and specimen preparation*

Cyclic (dynamic) bending moments were applied to lumbar–lumbar and lumbosacral joint complexes (containing three vertebral centra and two intervertebral discs each) of monkey (*Macaca fascicularis*), wallaby (*Wallabia rufogrisea fruticosa*), tiger (*Panthera tigris*), jaguar (*Panthera onca*) and seal (*Halichoerus grypus*). Following the static bending experiments, many more monkeys, wallabies and tigers (four, eight and three individuals respectively) were obtained. They were acquired from a primate research laboratory and Whipsnade Zoo, in the same manner as those obtained for the static bending experiments. The monkey and wallaby carcasses were dispatched directly to the department following culling, but the axial skeletons of the tiger carcasses were extracted by the author at the zoo and then transported back to Leeds. All individuals were used either immediately upon arrival at the laboratory or frozen for later use, well within 24 h

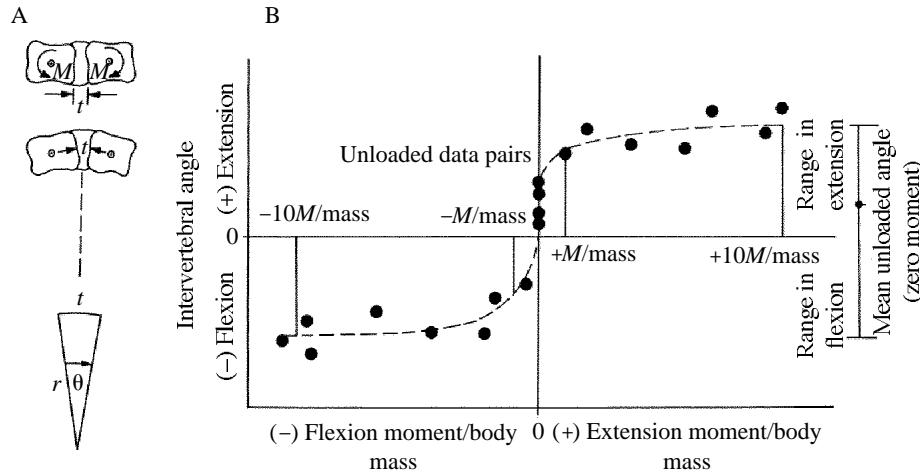


Fig. 3. When moments ( $M$ ) are applied to adjacent vertebrae, as shown in A, the angle between the two vertebrae ( $\theta$ ) may be expressed in terms of the thickness of the disc at the approximate centre of rotation ( $t$ ) and the radius of curvature ( $r$ ). The schematic diagram (B) illustrates how each data set from each joint of each species was analyzed. The angular differences between unloaded data pairs (extension and flexion angles at zero moment) were tested for significant neutral zones using paired Student's  $t$ -tests. Best-fitting curves (broken lines) were hand-drawn through the data, radiating from the mean of all unloaded angles. Absolute angular ranges in extension and flexion were measured from the mean unloaded angles to the asymptotic plateaus of these curves. To differentiate between bending behaviour at low and high bending moments, equal positive and negative specific bending moment ratios were located as shown, and intervertebral angles were taken from the estimates of joint behaviour (broken lines). Changes in intervertebral angle were measured from the mean unloaded angles to the broken lines at the appropriate ratios. See text for further explanation.

of death. The single jaguar specimen was obtained from Whipsnade Zoo in a similar manner to the tiger specimens. A different species of 'true' seal from that used for the static bending tests was obtained and used for the dynamic bending tests. It was caught in fishing nets and drowned. It was obtained by Dr Caroline Pond directly from the fishermen and forwarded to Leeds for immediate frozen storage. Again, all specimens were kept frozen at approximately  $-20^{\circ}\text{C}$ .

Vertebral columns were isolated as described in the previous section regarding the static bending experiments. Once dissected, they were cut into sections containing three vertebrae and two intervertebral discs. Holes were drilled through the central vertebrae at right angles to the sagittal (extension–flexion) plane, at the approximate vertical midpoints of the centra. Threaded steel bars (1/8 inch diameter for monkey and wallaby specimens, and 1/4 inch diameters for tiger, jaguar and seal specimens) were put through the holes. This unit was attached to the clamp. The clamp consisted of two right-angled steel brackets bolted together to make an arch. The threaded bar was inserted into slots and secured to the clamp with washers and nuts. The clamp and steel bar constituted a single rigid structure, while the specimen was allowed to rotate about the bar (see Fig. 4A).

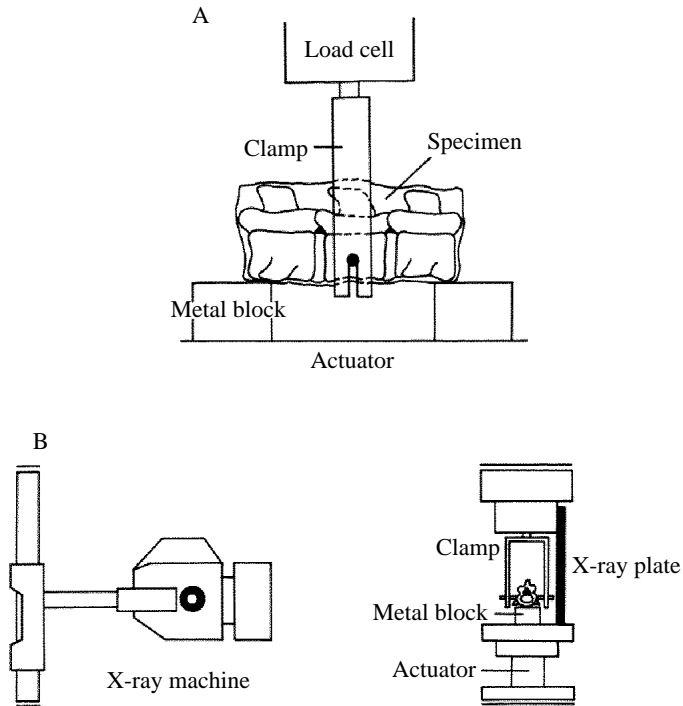


Fig. 4. The threaded steel bar is put through the central vertebra of the three-vertebrae/two-disc specimen shown in A. The bar is bolted to the metal clamp, which is attached to the load cell. The outer vertebrae sit on the metal blocks. The specimen is free to rotate about the steel bar. X-ray plates are positioned behind the specimen in the Instron testing machine, as shown in B. X-radiographs are taken at different stages in the bending cycle. See text for further explanation.

#### *The experimental set-up*

The specimen was then fixed to the load cell of the Instron dynamic testing machine (model 8031). The outer centra were placed upon metal blocks approximately equidistant from the central clamp (see Fig. 4A). When the actuator was set to oscillate, the specimen was subjected to three-point bending by virtue of the two contact points with the outer blocks and the central attachment to the clamp (the threaded bar). The amplitude of oscillation was chosen to maximize changes in intervertebral angle without damaging the specimen. A frequency of 0.5Hz was chosen as adequate and convenient for all specimens. Higher (>5Hz) and lower (0.1Hz) test frequencies did not appear to alter the characteristics of the resulting force traces (e.g. maximum forces, hysteresis loops). Specimens were cycled at least ten times (range 10–30 cycles) to remove any short-term creep effects. Force loops were generated for specimens in extension (dorsal concave or sagging) or flexion (dorsal convex or hogging) by flipping specimens over so that either the ventral surfaces of the vertebral centra, or the spinous processes, were in contact with the metal blocks. Specimens were lightly wrapped in cling-film and continually moistened with distilled water to prevent desiccation. This practice also served to reduce specimen–block friction to a minimum because the moistened specimen slid readily over

the cling-film covering the metal surface. In order to measure changes in intervertebral angle within the loop ranges, the machine was stopped at different points along the loop and X-radiographs were taken. Fig. 4B illustrates the relative position of the X-ray head to the specimen. Minimum head-to-specimen distances were 1.25m. X-ray plates were positioned approximately 10cm behind each specimen. A metal marker was placed in the plane of the specimen so that the X-ray dimensions could be corrected for magnification. X-ray exposure was calculated separately for each specimen, based on the mass of the animal from which it was obtained.

### *Theory and measurements*

The objective of these experiments was to measure the response of the intervertebral joints of different mammals to cyclic (dynamic) bending moments. The response was a change in the angle subtended by successive vertebrae. The energy input, or work associated with angular deformation, was also measured. All data required to make these calculations were derived from the force loops and the X-ray plates as follows.

*Bending moment and intervertebral angle.* For the purpose of these analyses, each test specimen was modelled as a freely supported beam with a single concentrated point load (Timoshenko and MacCullough, 1948). A diagram of the model is shown in Fig. 5A. A beam of total length  $L$  is supported on two triangular bases. The reaction forces associated with the points of contact between the triangular bases and the beam are  $R_1$  and  $R_2$ . A point load  $P$  is applied to the beam at a distance  $c$  from  $R_1$  and a distance  $d$  from  $R_2$ . The sum of  $c$  and  $d$  is equal to  $L$ , the total distance between the contact points. Consider the situation at equilibrium. Vertical forces must balance:

$$R_1 + R_2 = P$$

and the moments must be balanced. Solving for the moments about the reaction  $R_1$  gives:

$$R_2 L = Pc,$$

$$R_2 = Pc/L.$$

Similarly, balancing the moments about  $R_2$  gives:

$$R_1 = Pd/L.$$

Having solutions for the reactions at each support allows the calculation of the moments about any point along the beam. Consider the cross section OQ at a distance  $a$  from  $R_1$ . The bending moment about OQ can be calculated by summing all of the moments to either side of this cross section. Taking the moments to the left, one gets:

$$M_{OQ} = R_1 a,$$

$$M_{OQ} = Pad/L.$$

Fig. 5B shows a schematic diagram of an X-ray trace. Dimensions  $a$  and  $b$  are from the outer contact points with the metal block to the approximate geometric centres of the cranial and caudal intervertebral discs respectively.  $c$  and  $d$  are the distances between the contact points of the metal blocks to the central threaded bar. The central bar transmitted

the specimen force to the load cell *via* the clamp. By analogy with the beam drawing of Fig. 5A, the moments about the cranial and caudal disc centres would be:

$$M_{\text{cran}} = Pad/L$$

and

$$M_{\text{caud}} = Pbc/L$$

respectively. The forces ( $P$  values derived from the Instron force–displacement loops at each numbered exposure, see Fig. 5C), coupled with the dimensions described in Fig. 5B, were used to calculate the bending moments about each disc centre. Tracings were made of each X-ray plate, and a protractor was used to measure the angle between the central long axes of adjacent vertebrae. The error associated with using this technique to measure intervertebral angle was estimated by making ten tracings of two X-radiographs chosen at random. Joint angles were measured, and their mean values and standard errors were computed. The mean of the standard errors was chosen as a reasonable estimate of the potential measurement error. X-rays were taken at zero force first so that changes in angle could be related to increases in force and bending moment. Bending moment applied was divided by body mass to facilitate comparisons between animals of different sizes (see *The static bending experiments* section for the scaling arguments).

*Strain energy associated with bending the intervertebral joints.* A finite amount of energy is required to deform a solid. If the solid is a perfect spring, this deformation energy, or strain energy is completely recovered when the solid is allowed to return to its original state. Deforming a fluid also requires an input of energy. In contrast to a solid, a fluid does not return to its original condition following shear deformation, and no energy is recovered. Rather, the energy is lost as heat to the surroundings. Typically, the total energy applied to deform any material is not fully recovered when the deforming force is removed. The balance is lost as heat due to viscous shearing within the material itself. While the resilience (energy recovered/energy applied) of a steel spring is very nearly 100%, biological materials show much greater viscoelasticity, and as such are less resilient. Fig. 5C is a diagram of the Instron force–displacement output for a typical intervertebral joint complex bending test. Energy (or work) is the product of force and displacement. Therefore, the area below the upper curve of Fig. 5C (arrow showing increasing force) represents the work done by the Instron machine to bend the specimen. The area below the lower curve (arrow showing decreasing force) represents the release of strain energy by the specimen as it is allowed to return to its original shape. The discrepancy between these two curves, the enclosed loop, represents the energy lost to viscous processes.

At points 1, 2 and 3 (in Fig. 5C), X-rays were taken. At point 1, the force is zero, and the specimen is at rest. At points 2 and 3, the specimen has been bent, or deformed. The areas below the upper curve up to points 2 and 3 are measures of the energies associated with the angular deformation of both intervertebral joints and any energy absorbed by the steel bar or clamp. The compliances of the steel bars were measured by fitting them to the clamp as described in the experimental set-up. Three-point bending was applied to the threaded bars by forcing them against a half-inch brass bar mounted on the two metal blocks. The brass bar was positioned about the midpoint of the threaded bar in the same

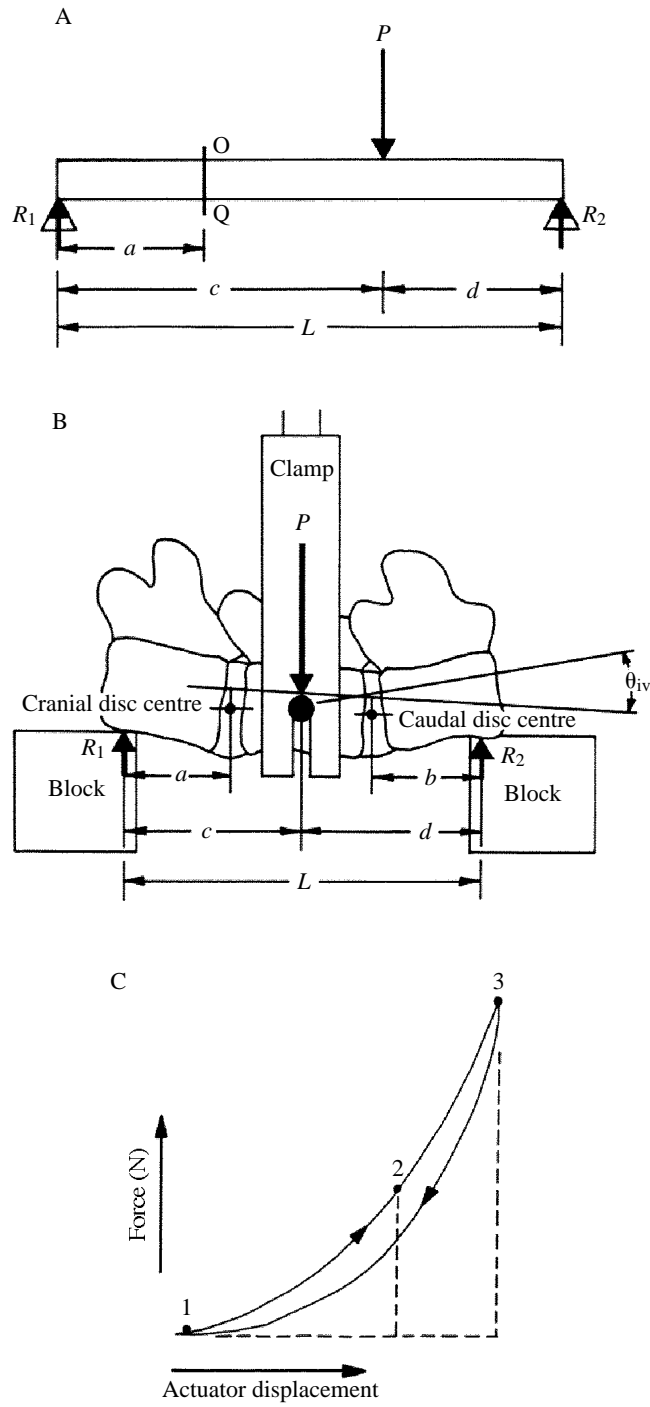


Fig. 5

Fig. 5. In A, three-point bending is applied to the beam by the force  $P$  and the reactions  $R_1$  and  $R_2$  at the triangular outer supports. The dimensions  $a$ ,  $b$ ,  $c$ ,  $d$  and  $L$  are required to calculate the bending moment about the cross-section OQ. By analogy with the beam in A, the bending moments about the cranial and caudal disc centres are calculated as shown in B. A schematic diagram of a force–displacement loop from a dynamic bending test is shown in C. The numbers 1–3 represent the points within the bending cycle where X-radiographs were taken. See text for further explanation.

way that each joint complex made contact with the threaded bar and the metal blocks. This brass bar was much stiffer than either of the threaded bars, so only compliances of the threaded bars were measured. The energies absorbed by the bars were subtracted from the total absorbed strain energies at each X-ray point, according to the forces measured by the load cell at each point. The balances were the energies absorbed by both intervertebral joints of each specimen. In order to quantify the work done to bend each joint, the following argument was used. If two identical Hookean springs suffer deformations in the ratio 1:2, then the loads (or in this case bending moments) are also in the ratio 1:2 and the strain energies are in the ratio 1:4. A square law was used. The strain energies were divided by body mass to facilitate comparisons among species on the basis of geometric similarity. If forces ( $F$ ) are applied to a Hookean solid, a deformation ( $\Delta\text{length}$ ) will occur. The work (energy) associated with such a deformation would be equal to  $1/2F(\Delta\text{length})$ . For geometrically similar objects at equal stress,  $\text{force} \propto \text{cross-sectional area} \propto \text{length}^2 \propto \text{mass}^{2/3}$ , and  $\Delta\text{length} \propto \text{length} \propto \text{mass}^{1/3}$ . Therefore,  $\text{work} \propto (\text{mass}^{2/3})(\text{mass}^{1/3})$ , or  $\text{energy} \propto \text{mass}$ . For geometrically similar joints, dividing the strain energy absorbed by body mass should yield a constant.

In this way, specific bending moments, changes in intervertebral angle and specific absorbed energies were calculated. Complete lumbar profiles were produced for the monkeys, wallabies and tigers (including the joint complexes cut from the single jaguar spine) by testing all combinations of lumbar–lumbar and lumbosacral joint complexes. As only one seal was available, a complete profile of the lumbosacral sagittal bending behaviour was not possible. Only uppermost and lowermost joints were tested.

#### *Data analyses and statistics*

Changes in intervertebral angle were plotted as functions of applied bending moment/body mass separately for the extension and flexion of each joint of each animal group. The static bending data obtained for these species were included in these analyses because cycling frequency appeared to have had little effect on the force–displacement output. Since many of the static data were concerned with the forced angular ranges, their inclusion enhanced the identification of the asymptotic plateaus ( $A$  values described in the model below).

Typically, intervertebral angles increased (positively if extending or negatively if flexing) with increasing applied specific moment, until some plateau was reached. Further deformation would have ultimately caused joint failure, and was avoided. The bending data were therefore modelled as negative exponential functions of the form:

$$y = A(1 - e^{-Bx}),$$

where  $x$  values were bending moment/body mass and  $y$  values were the observed changes in intervertebral angle. The Statistical Analysis System (SAS) non-linear procedure and/or Biomedical Computer Programs (BMDP) non-linear procedure were used to calculate  $A$  and  $B$  and their standard errors for each joint in extension and flexion.  $A$  was the asymptotic plateau of the joint and was similar to the forced bending range described in *The static bending experiments* section.  $B$  was the rate constant of each function, describing how quickly the joint reached the plateau. It was essentially a measure of joint compliance. The lower the  $B$  value, the more stiff the joint would be in the particular bending direction.

Two questions were considered: (1) whether lumbar–lumbar and lumbosacral joint parameters within species were sufficiently similar to warrant representation by single pooled functions, and (2) whether homologous joint parameters of all species were sufficiently similar to warrant representation by single pooled functions. Chow's test (Dillon and Goldstein, 1984) was used to compare the residual sum of squares resulting from combining data into single pooled functions, and the separate functions for each joint:

$$Q = \frac{[(SSE_{\text{pool}} - \sum SSE_{\text{ind}})/k]}{[\sum SSE_{\text{ind}}/(n_{\text{tot}} - mk)]},$$

where  $SSE_{\text{pool}}$  was the residual sum of squares when groups of data were pooled into single functions,  $SSE_{\text{ind}}$  was the residual sum of squares when groups of data were considered as individual functions,  $k$  was the number of parameters,  $n_{\text{tot}}$  was the number of data points combined from all groups and  $m$  was the number of individual groups. Since  $Q$  and  $F$  distributions are approximately equal (Dillon and Goldstein, 1984), the following decision rule was used. If  $Q > F_{\alpha.05}$  (d.f. are  $k, n_{\text{tot}} - mk$ ), the null hypothesis, that all the data were best represented by a single function, was rejected. The alternative hypothesis, that all the data were sufficiently different to warrant separate functions, was accepted.

The specific strain energies absorbed for the observed changes in intervertebral joint angle were pooled within species groups for joints with similar bending plateaus and compliances ( $A$  and  $B$  values respectively). As intervertebral angles increased, the strain energies absorbed increased non-linearly. The energy data were therefore modelled as power functions of the form:

$$y = Cx^D,$$

where  $x$  values were the observed changes in intervertebral angle, and  $y$  values were the corresponding specific strain energies absorbed by the joints. The SAS general linear model procedure and/or Biomedical Computer Programs (BMDP) linear regression procedure were applied to each set of log-transformed data to calculate  $\log C$  and  $D$  values and their standard errors.  $D$  would be 2 for Hookean springs. Non-linear biological springs might be expected to have exponents greater than 2.  $\log C$  values indicated the capacities of the intervertebral joints for absorption of strain energy. Strain energy functions were compared using Chow's test, as described above, to decide whether the absorption of strain energies by joints from different species could be represented by single pooled functions or would require consideration separately.

Intervertebral joint resilience was defined as the percentage recovery of elastic strain energy:

$$\frac{(\text{strain energy released})}{(\text{strain energy absorbed})} \times 100.$$

Only those strain energies released and absorbed at the maximally recorded forces of the force–displacement loops (see Fig. 5C, point 3, for example) were used to calculate resiliences. These calculations were corrected for the compliances of the threaded bars, and the mean values (of different joints within the joint pools) were recorded where possible.

## Results

### *The static bending experiments*

Table 1 shows the percentage of total body mass devoted to the major lumbar extensors and flexors. The greatest disparity between the two was in the wallaby, with 8.2 and 0.7 % respectively. Extension and flexion muscles were more equally proportioned in the monkey, at 3.2 and 1.3% respectively. The largest back extensor in all species was longissimus (often called longissimus et iliocostalis or longissimus dorsi). It originated on the iliac crest and continued over the lumbar to the base of the skull. In sheep (and tiger) slips diverged from the main muscle mass to terminate on the dorsal aspect of the ribs and cervical vertebrae (Getty, 1975). Multifidus was difficult to distinguish in these species. In monkey, rabbit and wallaby, the longissimus muscle appeared to be more segmented over the lumbar, and the multifidus was more prominent than in the other species. The main lumbar flexors were the psoas (major and minor) muscles. These were always less substantial than the lumbar extensors in all species. Since the seal (*Phoca vitulina*) was an incomplete specimen, no total muscle masses could be determined.

Significant neutral zones were measured in the lumbosacral joints of rabbit, wallaby, badger and seal [about 11, 5, 7 and 18° (absolute values) respectively]. Lumbar–lumbar neutral zones were only significant in the seal and in some of the rabbit joints [about 16 and 2° (absolute values) respectively].

Table 1. *Body masses and percentage extensor and flexor muscle masses in the experimental species*

Animal	Body mass (kg)	Extensors (% body mass)	Flexors (% body mass)
Monkey	2–3	3.2	1.3
Rabbit	2.5–5.5	5.6	1.1
Badger	8	4.0	0.6
Wallaby	4–12	8.2	0.7
Sheep	50–60	2.7	0.6
Tiger	100	5.4	0.9

The total body mass and percentage body mass occupied by major lumbar extensors and flexors of each experimental species is shown, where complete muscle dissections were possible. See text for further explanation.

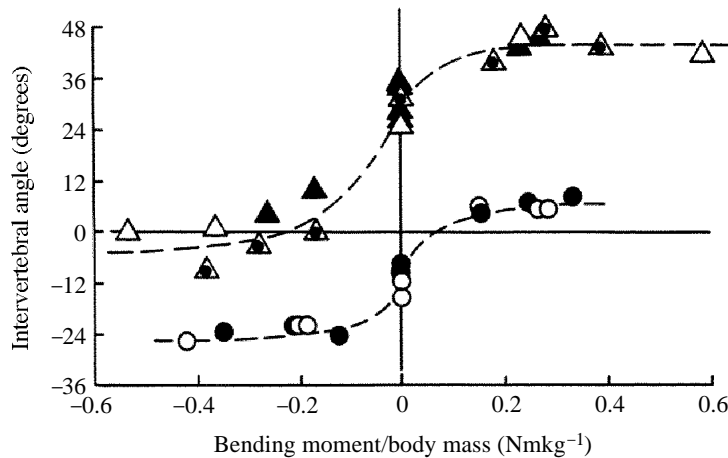


Fig. 6. The raw bending data from the upper lumbar–lumbar joint (L1L2) of two badgers (8.1kg, ○, and 8.8kg, ●) and from the lumbosacral joints of three wallabies (12kg, ▲, 5.5kg, △, and 4.4kg, ◐) are shown with the best-fitting hand-drawn curves (broken lines) radiating from the mean of the unloaded joint angles of each species. See text for further explanation.

Fig. 6 shows samples of the raw data from badger upper lumbar (L1L2) and wallaby lumbosacral (L6S) joints. Best-fitting hand-drawn curves are shown radiating from the mean of all of the unloaded intervertebral angles for each species group. The error associated with measuring intervertebral angle by the X-radiograph and protractor technique used here was about  $\pm 1.5^\circ$ .

A summary of the forced angular ranges is shown in Fig. 7. Lumbar–lumbar joints had similar ranges within any species and generally lower capacities for bending than the lumbosacral joints. The contrast between the bending capacity of lumbar–lumbar and lumbosacral joints was particularly prominent in the sheep. Because the length of the tiger's column exceeded that of the large X-ray plates, the X-rays were focused upon the middle to lower lumbar region. Although measurements for upper lumbar joints were not possible, visual inspections of the bent columns suggested that the upper lumbar joints behaved similarly to the lower lumbar joints. Extension plateaus for the seal and tiger joints could not be determined because the plateaus were not obvious from the extension data available.

Fig. 8 illustrates the relative bending behaviour of all of the experimental species. Here, geometric similarity is considered (see Materials and methods, *The static bending experiments* section for the scaling arguments) and the applied bending moments have been divided by body mass. Monkey joints were remarkably resistant to sagittal bending, relative to their size. The seal lumbar–lumbar joint was particularly conspicuous for its very low sagittal bending resistance.

#### *The dynamic bending experiments*

Fig. 9 shows the bending results and corresponding negative exponential function for wallaby midlumbar (L3L4) joints in flexion. The error associated with measuring

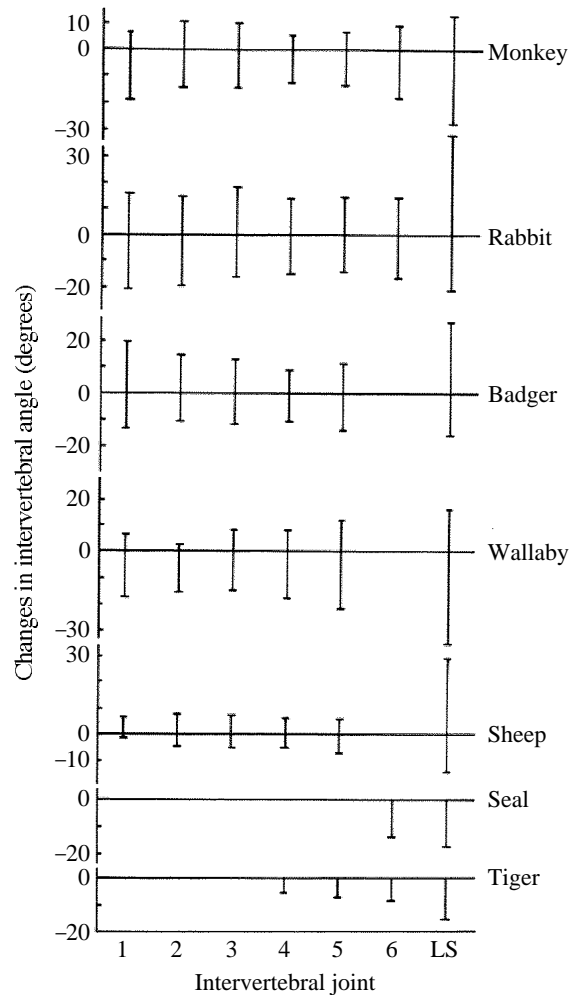


Fig. 7. The angular bending ranges in extension and flexion (positive and negative values respectively) are shown for each experimental species. Numbers 1, 2, 3, 4, 5 and 6 represent joints L1L2, L2L3, L3L4, L4L5, L5L6 and L6L7, respectively, and LS, lumbosacral joint. The tiger column length exceeded the length of the large X-ray plate, so only the middle and lower lumbar joints are shown. Extension plateaus were not obvious for the seal or tiger, given the applied bending moments. See text for further explanation.

intervertebral angles during the dynamic bending tests, about  $\pm 1^\circ$ , was lower than that associated with the static bending tests ( $\pm 1.5^\circ$ , as previously stated).

Tables 2–5 show the *A* and *B* values and their standard errors for each joint of each species group. *F* values indicate the goodness of fit of the models. Table 6 summarizes the results of Chow's tests for comparisons between intervertebral joints within species groups. The null hypothesis was rejected in every comparison. A visual inspection of the bending joints within species suggests that differences, particularly between lumbar–lumbar and lumbosacral joints, were primarily due to their bending capacities (*A*

values). The  $B$  values (compliances) of the joints of land mammals typically had large standard errors in extension, but were clearly conserved between joints in flexion.

Fig. 10 illustrates homologous joint comparisons of the four species groups; the

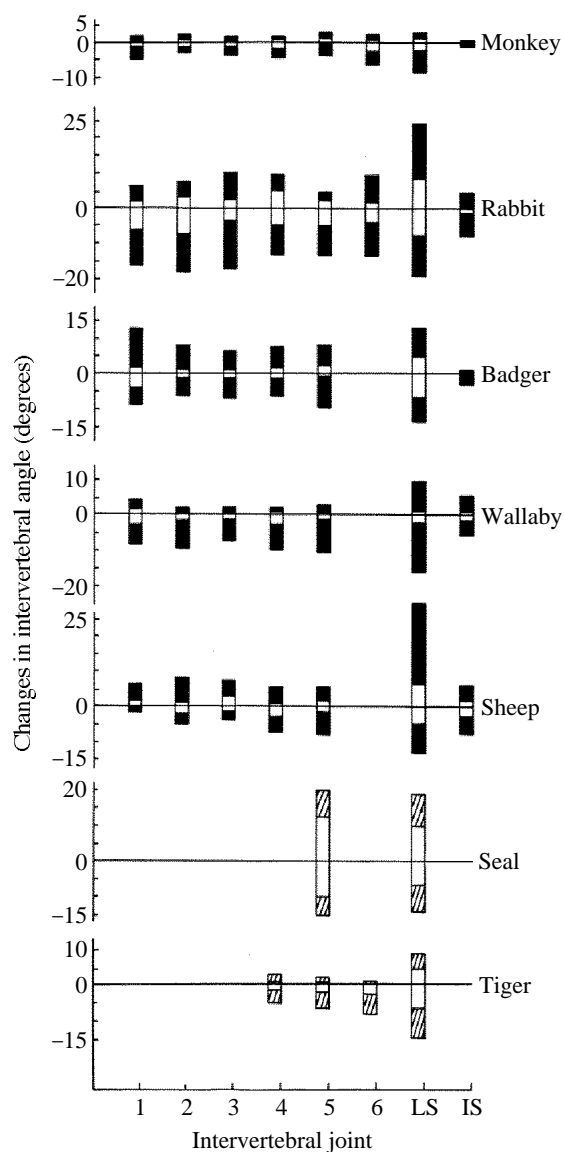


Fig. 8. Changes in intervertebral angle with the application of low specific extension and flexion moments ( $\pm 0.01 \text{ Nm kg}^{-1}$ ) are shown for all species by the open bars. The changes in intervertebral angle with the application of high specific extension and flexion moments are indicated by the open bars plus the filled bars ( $\pm 0.10 \text{ Nm kg}^{-1}$ , for monkey, rabbit, badger, wallaby and sheep) or the cross-hatched bars ( $\pm 0.05 \text{ Nm kg}^{-1}$  for the seal and tiger). Numbers 1, 2, 3, 4, 5 and 6 represent joints L1L2, L2L3, L3L4, L4L5, L5L6 and L6L7 respectively. LS, lumbosacral joint; IS, iliosacral joint. See text for further explanation.

lumbosacral joints in extension and the upper lumbar joints (L1L2 and L2L3) in flexion. The extension capacities of the joints of land mammals ( $A$  values) were typically much lower than those for the semi-aquatic seals (*Phoca vitulina* and *Halichoerus grypus*).

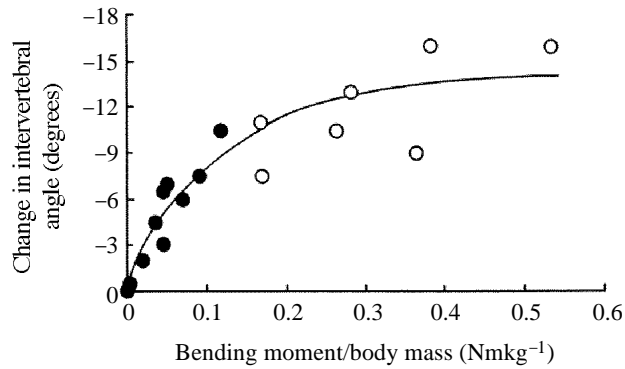


Fig. 9. The observed changes in intervertebral angle with the application of dynamic (●) and static (○) bending moments are shown for wallaby L3L4 joints in flexion. The least-squares best-fitting negative exponential function is shown by the solid line:  $\theta_{iv} = -13.5[1 - e^{-9.1(M/mass)}]$ . See text for further explanation.

Table 2. The negative exponential model parameters for monkey joints in extension and flexion

Joints	A (degrees)	S.E.	B (kgNm <sup>-1</sup> )	S.E.	F	N	Range of $\Delta\theta_{iv}$ (degrees)
Extension							
L1L2	+5	0.42	24.6	15.4	89.6	14	+2 to +7
L2L3	+6.5	0.45	18.6	6.8	130.7	14	+4 to +8
L3L4	+5	0.42	$4.7 \times 10^{10}$	—	158.4	12	+2.5 to +7.5
L4L5	+4.1	0.61	21.2	52.5	30.7	11	+2 to +6.5
L5L6	+6.4	0.51	31.1	9.4	109.0	14	+2.5 to +8
L6S	+9.6	0.88	16.0	4.8	78.4	13	+3.5 to +14
Flexion							
L1L2	-16.1	1.00	6.0	1.9	151.8	16	-2.5 to -21.5
L2L3	-12.3	0.99	2.6	0.8	287.9	17	-1 to -14.5
L3L4	-14.5	1.83	2.4	1.1	201.4	13	-1.5 to -15.5
L4L5	-11.4	0.61	3.7	1.4	469.2	13	-1.5 to -12.5
L5L6	-10.3	0.63	19.2	6.7	144.6	14	-2.5 to -14
L6S	-23.1	1.56	4.2	1.6	184.9	15	-5 to -26.5

Changes in intervertebral angle from the unloaded excised state ( $\Delta\theta_{iv}$ ) were modelled as functions of specific bending moment ( $M/mass$ ),  $\Delta\theta_{iv} = A(1 - e^{-BM/mass})$  for monkey lumbar–lumbar and lumbosacral joints in extension and flexion.

$A$  and  $B$ , the asymptotic plateau and the rate at which the plateau is reached, respectively, are presented for each joint in each direction of bending, with their standard error.

The high  $F$  values indicate the significance of the models.

The sample sizes are indicated by  $N$  values.

See text for further explanation.

Table 3. *The negative exponential model parameters for wallaby joints in extension and flexion*

Joints	A (degrees)	S.E.	B (kgNm <sup>-1</sup> )	S.E.	F	N	Range of $\Delta\theta_{iv}$ (degrees)
Extension							
L1L2	+5.9	0.94	604.9	–	39.2	8	+3.5 to +11
L2L3	+3.8	0.46	28.8	15.7	54.6	15	+1 to +6
L3L4	+5.9	1.36	6.9	3.8	41.8	17	+1 to +7
L4L5	+4.6	0.51	21.1	14.1	60.5	11	+2 to +5.5
L5L6	+5.2	0.82	1249.7	–	40.6	16	+1 to +11
L6S	+8.4	2.39	12.3	9.5	24.8	10	+3 to +13
Flexion							
L1L2	–15.9	2.61	12.9	7.2	49.0	7	–6.5 to –18.5
L2L3	–15.2	1.79	10.5	2.6	151.9	15	–1.5 to –18.5
L3L4	–13.5	1.24	9.1	2.2	157.7	16	–2 to –16
L4L5	–14.5	1.20	24.6	15.3	82.3	9	–7 to –19
L5L6	–18.4	0.92	15.7	2.5	314.8	17	–2 to –22.5
L6S	–29.7	1.52	14.5	2.4	322.2	17	–9 to –38

Changes in intervertebral angle from the unloaded excised state ( $\Delta\theta_{iv}$ ) were modelled as functions of specific bending moment ( $M/\text{mass}$ ),  $\Delta\theta_{iv}=A(1-e^{-BM/\text{mass}})$  for wallaby lumbar–lumbar and lumbosacral joints in extension and flexion.

$A$  and  $B$ , the asymptotic plateau and the rate at which the plateau is reached, respectively, are presented for each joint in each direction of bending, with their standard error.

The high  $F$  values indicate the significance of the models.

The sample sizes are indicated by  $N$  values.

See text for further explanation.

Extension compliances ( $B$  values) for seal joints were much greater than those for the other groups. Flexion capacities and compliances differed for each species group. Monkey and wallaby joints were typically stiffer (lower  $B$  values) than tiger/jaguar joints and had greater capacities (higher  $A$  values) for flexion. Seal joints were very compliant (high  $B$  values) relative to all terrestrial species (see Tables 2–5 for details). Table 7 summarizes the results of the Chow's tests for comparisons of homologous joints in extension and flexion. Joint bending parameters were sufficiently different to warrant description by separate functions in all comparisons except for homologous midlumbar (L3L4 and L4L5) joints in extension (indicated by the asterisks), where the null hypothesis was accepted in each case. These comparisons involved only the terrestrial species.

Fig. 11 shows an example of the pooled energy data and corresponding power curve for the tiger and jaguar joints in extension. Joints with similar bending plateaus and compliances ( $A$  and  $B$  values, respectively, effectively all lumbar–lumbar joints within the species groups) were pooled and used to calculate the coefficients and the exponents ( $C$  and  $D$  values respectively) of the power curves shown in Table 8. Seal joints showed particularly low capacities for absorbing strain energy (low  $C$  values) in both extension and flexion, compared to the joints of land mammals. Chow's test results (also included in

Table 4. *The negative exponential model parameters for tiger and jaguar joints in extension and flexion*

Joints	A (degrees)	S.E.	B (kgNm <sup>-1</sup> )	S.E.	F	N	Range of $\Delta\theta_{iv}$ (degrees)
Extension							
L1L2	+4.7	0.20	91.8	29.5	361.4	10	+3.5 to +5.5
L2L3	+7.9	0.26	19.5	1.5	$2.7 \times 10^4$	4	+5.5 to +6.5
L3L4	+3.5	0.35	58.4	44.0	82.3	7	+2.5 to +4
L4L5	+3.1	0.36	63.2	69.6	72.8	9	0 to +4.5
L5L6	+2.9	0.46	2167.1	—	39.9	7	+1.5 to +4.5
L6L7	+6.0	0.99	55.5	26.1	70.5	12	+1.5 to +7
L7S	+8.4	0.90	25.0	5.1	354.8	10	+2 to +7.5
Flexion							
L1L2	-9.6	0.58	98.7	49.2	255.6	8	-7.5 to -11
L2L3	-7.9	0.37	1182.6	—	453.5	5	-7 to -9
L3L4	-6.2	0.24	94.0	22.4	990.9	6	-5.5 to -6.5
L4L5	-4.9	0.33	50.8	12.9	590.9	9	-3.5 to -5
L5L6	-6.7	1.66	64.8	99.4	67.9	6	-4.5 to -8
L6L7	-8.5	0.54	89.5	22.4	221.6	12	-1 to -9.5
L7S	-11.2	1.06	46.6	13.5	177.4	9	-2 to -12

Changes in intervertebral angle from the unloaded excised state ( $\Delta\theta_{iv}$ ) were modelled as functions of specific bending moment ( $M/\text{mass}$ ),  $\Delta\theta_{iv}=A(1-e^{-BM/\text{mass}})$  for tiger and jaguar lumbar–lumbar and lumbosacral joints in extension and flexion.

A and B, the asymptotic plateau and the rate at which the plateau is reached, respectively, are presented for each joint in each direction of bending, with their standard error.

The high F values indicate the significance of the models.

The sample sizes are indicated by N values.

See text for further explanation.

Table 8) show that specific strain energy parameters for each species were sufficiently different to merit the rejection of the null hypothesis, that strain energy absorption behaviour could be described by single pooled functions.

Resiliences are also summarized in Table 8. Extension resiliences of the joints of land mammals were similar to each other (about 67–75%) and greater than those of the seal joints (about 48%). Flexion resiliences of monkey and wallaby joints were similar to each other (about 65–67%) and much greater than tiger/jaguar and seal values (36 and 41% respectively).

### Discussion

The neutral zone of a joint is the range of unloaded or unforced mobility. Low-friction joints typically have substantial neutral zones (the wrist, for example). Yamamoto *et al.* (1989) quantified neutral zones in cadaveric human lumbar–lumbar and lumbosacral joints. Pure bending moments were applied to *post mortem* lumbosacral spines with a specially designed loading jig. Intervertebral angles were measured by stereophotogrammetry of special markers on each vertebra. They found statistically significant neutral zones in both the lumbar–lumbar and lumbosacral joints (mean values

Table 5. *The negative exponential model parameters for seal joints in extension and flexion*

Joints	A (degrees)	S.E.	B (kgNm <sup>-1</sup> )	S.E.	F	N	Range of $\Delta\theta_{iv}$ (degrees)
Extension							
L1L2	+17.3	2.22	266.1	79.7	65.9	7	+4.5 to +18
L2L3	+14.8	1.32	512.1	160.6	109.4	7	+7 to +18
L5L6	+19.3	0.91	154.2	21.8	291.1	9	+3 to +20.5
L6S	+17.0	1.19	253.7	64.1	172.9	9	+9 to +19.5
Flexion							
L1L2/L2L3	-12.6	1.09	398.8	67.1	244.1	10	-4.5 to -12
L5L6	-13.6	1.10	282.7	82.0	111.1	9	-5 to -16.5
L6S	-10.2	0.72	334.3	91.5	139.7	9	-3.5 to -12.5

Changes in intervertebral angle from the unloaded excised state ( $\Delta\theta_{iv}$ ) were modelled as functions of specific bending moment ( $M/\text{mass}$ ),  $\Delta\theta_{iv}=A(1-e^{-BM/\text{mass}})$  for seal lumbar–lumbar and lumbosacral joints in extension and flexion.

$A$  and  $B$ , the asymptotic plateau and the rate at which the plateau is reached, respectively, are presented for each joint in each direction of bending, with their standard error.

The high  $F$  values indicate the significance of the models.

The sample sizes are indicated by  $N$  values.

See text for further explanation.

Table 6. *Q values for comparisons of joints within species*

	Q	d.f.	P value
Monkey, extension (L1L2L3L4L5L6S)	18.0	2, 65	0.0000
Monkey, flexion (L1L2L3L4L5L6S)	74.1	2, 72	0.0000
Wallaby, extension (L1L2L3L4L5L6S)	20.5	2, 66	0.0000
Wallaby, flexion (L1L2L3L4L5L6S)	175.4	2, 74	0.0000
Tiger/jaguar, extension (L1L2L3L4L5L6L7S)	18.6	2, 47	0.0000
Seal, extension (L1L2L3L5L6S)	9.6	2, 23	0.0009
Seal, flexion (L1L2L3L5L6S)	8.2	2, 26	0.0017

The results of Chow's test, comparing intervertebral joints within species groups, are summarized.

Since all  $P$  values are less than 0.05, the null hypotheses are rejected and the alternative hypotheses are accepted.

See text for further explanation.

and standard errors typically less than 2 and  $\pm 0.5^\circ$  and less than 3 and  $\pm 0.7^\circ$  respectively). These neutral zones, particularly for the lumbosacral joints, were much smaller than those measured for the mammals of this study. However, the error associated with measuring intervertebral angles by their method was  $\pm 0.2^\circ$ , compared to an error of about  $\pm 1.5^\circ$  here. Although they also used four-point bending to apply pure static moments, their loading and angle measurement systems were much more sophisticated than those used in the first part of this study. Their motives were specifically related to determining the magnitudes of joint movement in human intervertebral joints in health and disease. Clinical diagnoses of spinal pathologies depend upon detailed knowledge of the normal

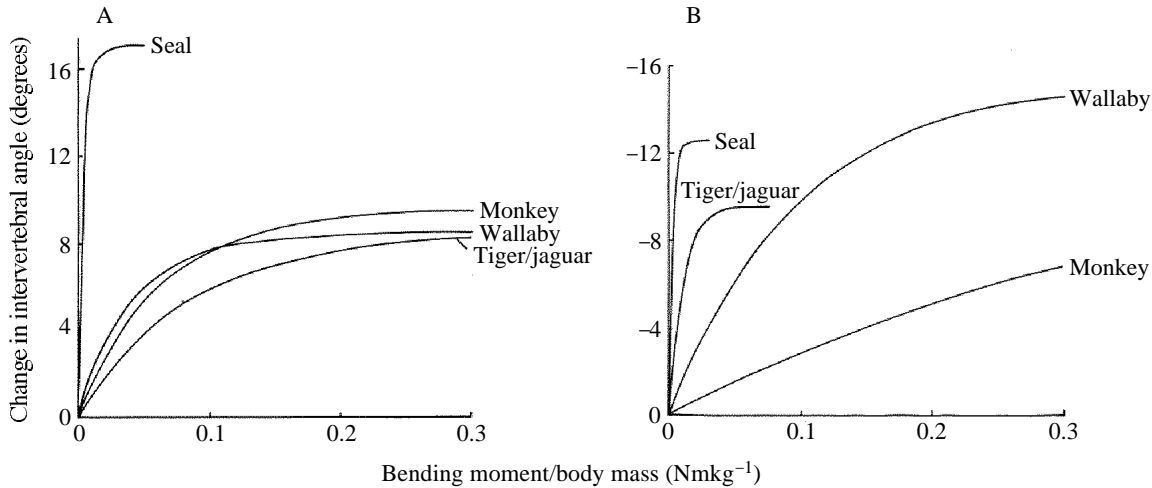


Fig. 10. (A) The negative exponential functions for extending lumbosacral joints of each species group: monkey,  $\Delta\theta_{iv}=9.6[1-e^{-16.0(M/mass)}]$ ; wallaby,  $\Delta\theta_{iv}=8.4[1-e^{-12.3(M/mass)}]$ ; tiger/jaguar,  $\Delta\theta_{iv}=8.4[1-e^{-25.0(M/mass)}]$ ; seal,  $\Delta\theta_{iv}=17.0[1-e^{-253.7(M/mass)}]$ . (B) The negative exponential functions for the flexing upper lumbar–lumbar joints of each species group: monkey (L2L3),  $\Delta\theta_{iv}=-12.3[1-e^{-2.6(M/mass)}]$ ; wallaby (L2L3),  $\Delta\theta_{iv}=-15.2[1-e^{-10.5(M/mass)}]$ ; tiger/jaguar (L1L2),  $\Delta\theta_{iv}=-9.6[1-e^{-98.7(M/mass)}]$ ; seal (L1L2/L2L3),  $\Delta\theta_{iv}=-12.6[1-e^{-398.8(M/mass)}]$ .

Table 7. *Q values for comparisons of homologous joints between species*

	<i>Q</i>	d.f.	<i>P</i> value
L1L2 extension (MWT/JS)	61.5	2, 31	0.000
L2L3 extension (MWT/JS)	109.4	2, 32	0.000
L3L4 extension (MWT/J)	0.28	2, 30	0.758*
L4L5 extension (MWT/J)	3.0	2, 25	0.068*
L5L6 extension (MWT/JS)	69.6	2, 38	0.000
L6S extension (MWT/JS)	156.2	2, 40	0.000
L1L2 flexion (MWT/JS)	16.22	2, 32	0.000
L2L3 flexion (MWT/JS)	67.8	2, 34	0.000
L3L4 flexion (MWT/J)	8.3	2, 31	0.001
L4L5 flexion (MWT/J)	24.0	2, 25	0.000
L5L6 flexion (MWT/JS)	47.9	2, 39	0.000
L6S flexion (MWT/JS)	87.4	2, 42	0.000

The results of Chow's test, comparing homologous intervertebral joints between species groups, are summarized.

The null hypotheses are accepted where *P* values are greater than 0.05 (marked with an asterisk).

Mid-lumbar joints of the terrestrial species groups (L3L4 and L4L5) did not show significantly different extension behaviour to warrant description by separate functions.

See text for further explanation.

M, monkey; W, wallaby; T, tiger; J, jaguar; S, seal.

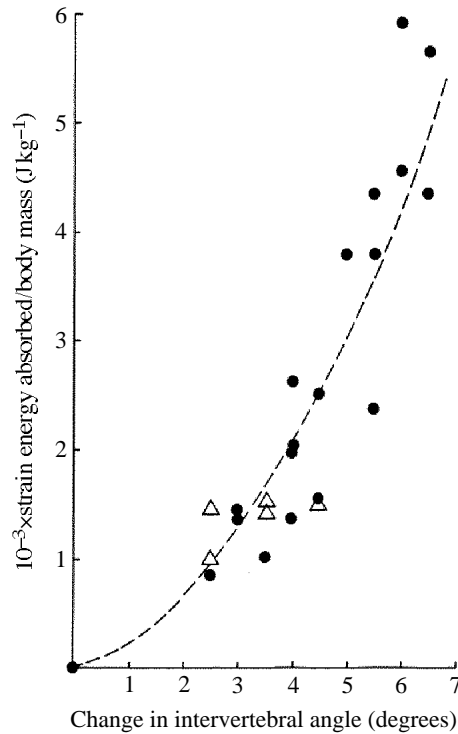


Fig. 11. The specific strain energies absorbed by extending tiger (●) and jaguar (△) lumbar–lumbar joints are modelled as a power function of the applied changes in intervertebral angle:  $E_{IN}/\text{mass} = 2.10 \times 10^{-4} (\Delta\theta_{IV})^{1.66}$  (broken line). See text for further explanation.

healthy state of intervertebral joints, so accuracy is extremely important. Exploring the trends and patterns of mammalian intervertebral mobility was the motive for this study, so extreme accuracy was less important. Nonetheless, the neutral zone of human lumbosacral joints appears to be less than those of the other mammalian species studied here.

The forced extension and flexion ranges were determined from the mean of all of the unloaded intervertebral angles to give approximate plateau angles (see Fig. 3B). Given that the measurement accuracy per angle was about  $\pm 1.5^\circ$ , forced ranges determined from the difference between two angles should be expected to have a greater associated error. Therefore, the forced ranges of motion of monkey, rabbit, badger and wallaby lumbar–lumbar joints were not clearly different (see Fig. 7). Sheep and tiger lumbar–lumbar ranges (tiger in flexion only) were similar, yet noticeably smaller than those of other terrestrial mammals. Lumbosacral joints had greater forced ranges than lumbar–lumbar joints in all species, with the greatest contrast between the two in the sheep. Yamamoto *et al.* (1989) also measured the range of movement of the human lumbar column. They subjected lumbosacral spines to a maximum of 10Nm, stating that this achieved the greatest movement, without causing structural damage. Values ranged from 4.3 to 5.8° and 5.8 to 8.9° for lumbar–lumbar extension and flexion, respectively,

Table 8. The power curve coefficients and exponents for each species in extension and flexion

Animal joints	C						Resilience	
	logC	s.E.	(Jkgdegree <sup>-1</sup> )	D	s.E.	r <sup>2</sup>	N	(%)
Extension								
Monkey (L1L2L3L4L5)	-3.060	0.245	8.71×10 <sup>-4</sup>	1.55	0.40	0.72	9	75
Wallaby (L1L2L3L4L5L6)	-3.302	0.142	4.99×10 <sup>-4</sup>	1.63	0.34	0.75	11	69
Tiger/jaguar (L1L2L3L4L5L6L7)	-3.677	0.102	2.10×10 <sup>-4</sup>	1.66	0.17	0.82	25	67
Seal (L1L2L3L5L6S)	-5.574	0.208	2.67×10 <sup>-6</sup>	1.96	0.21	0.82	21	48
Flexion								
Monkey (L1L2L3L4L5)	-3.262	0.170	5.47×10 <sup>-4</sup>	1.58	0.54	0.47	13	65
Wallaby (L1L2L3L4L5)	-3.444	0.141	3.60×10 <sup>-4</sup>	1.55	0.18	0.90	11	67
Tiger/jaguar (L1L2L3L4L5L6L7)	-4.335	0.206	4.62×10 <sup>-5</sup>	2.18	0.24	0.85	17	36
Seal (L1L2L3L5L6S)	-4.855	0.144	1.40×10 <sup>-5</sup>	1.78	0.17	0.87	19	41

The specific strain energies absorbed by intervertebral joints ( $E_{IN}/\text{mass}$ ) were modelled as power functions of changes in intervertebral angle ( $\Delta\theta_{iv}$ , from the unloaded excised states),  $E_{IN}/\text{mass} = C(\Delta\theta_{iv})^D$ , for each animal group.

Data from all joints with similar bending plateaus ( $A$  values) were pooled within each animal group for each direction of bending (see Table 7).

$C$  and  $D$  values, with their standard errors, are shown.

The  $r^2$  values indicate the goodness of fit of the models, and the  $N$  values indicate the sample size.

The approximate percentage resiliences of the joints are shown in the last column.

$Q$  values for Chow's tests of extension and flexion energy comparisons ( $Q=929.2$ , d.f.=2, 104 and  $Q=135.2$ , d.f.=2,76, respectively) give  $P$  values less than 0.05 that result in the rejection of the null hypotheses.

See text for further explanation.

and 7.8 and 10° for lumbosacral joints in extension and flexion respectively. These values are noticeably lower than those for the animals in the static bending portion of this report, especially with respect to the lumbosacral joint (see Fig. 7). The sheep and tiger appear to have similarly reduced mobility in the lumbar–lumbar joints, but relatively enhanced mobility in the lumbosacral joint.

Range of movement has been measured in the intervertebral joints of horses by several investigators. Jeffcott and Dalin (1980) performed three-point bending tests with horse thoracolumbar spines. Specimens were freely supported at each end and a 10kg weight was hung from a point along the length near the midpoint (T12–T13). To reverse the moment, the specimens were suspended from these midpoints such that the end supports were free of load. They found very low lumbar–lumbar mobility compared to highly mobile lumbosacral joints. Unfortunately, their technique did not apply a constant moment over the region of the column in question. In three-point bending of beams with freely supported ends, the bending moment diminishes from a maximum at the point of force application to zero at the free ends (Timoshenko and MacCullough, 1948). It is likely that some of their experimental joints experienced very low bending moments and therefore would tend to bend very little. Townsend *et al.* (1983) also studied the kinematics of the equine thoracolumbar spine. The sacral ends of specimens were clamped in a vice and the thoracic ends were manually bent until no further movement between the joints occurred. Each specimen was treated as a cantilever beam. In such a

system, the applied bending moment increases from zero at the free (thoracic) end to a maximum at the clamped (sacral) end. It is not surprising, therefore, that they found the greatest scope for extension and flexion in the lumbosacral joint. Since the force was applied manually, the maximum bending moment cannot be estimated. Slijper (1946) estimated the dorsoventral mobility of several mammals including kangaroo and monkey. He bent the carcasses in flexion and extension and traced the subsequent body profiles. Again, detailed information about the forces and/or moments applied was not given. The clear benefit of using a four-point bending technique is that a uniform or pure moment is applied to every joint along the column. This facilitates joint-by-joint comparisons within each column and between individuals within and among species groups.

Smeathers (1981) observed that small animals tended to have long arched flexible lumbar vertebral columns, whereas larger animals' columns tended to be rather shorter and more rigid. He suggested that, although flexible spines would require considerable muscular effort to maintain posture, they would be relatively easy to move. Mass scales as length<sup>3</sup>, but muscle force (proportional to cross-sectional area) scales as length<sup>2</sup>. Therefore, relatively more muscle is required by a large animal to exert a force that is of the same multiple of body mass as in a small animal. Smeathers suggested that larger animals would benefit from having relatively rigid backs. Posture could be maintained passively, at the expense of an enhanced cost associated with bending the spine. Certainly, the smaller animals of this study had greater capacities for joint (particularly lumbar–lumbar) movement. However, this argument does not offer any energetic reasons for the apparent lack of small stiff-backed animals. Surface area to volume ratios increase with decreasing animal size. Perhaps a flexible spine, one with a more even distribution intervertebral joint mobility, is important for small animals because it allows them to curl up. By approximating a spherical shape, they could minimize their surface area to volume ratio and reduce heat loss. Thermoregulation is an important aspect of small mammal physiology, and it seems likely that any adaptive feature allowing them to enhance their capacity for heat retention would be beneficial.

The marked differences between the forced bending ranges of the lumbar–lumbar and lumbosacral joints in some larger quadrupeds (sheep in this study and horses in Jeffcott and Dalin, 1980, and Townsend *et al.* 1983) perhaps reflect a change in the function of the lumbosacral joint from a supporting joint to a locomotor joint. The supraspinous ligament does not cross the lumbosacral joint in many of these animals (Slijper, 1946; Getty, 1975). The supraspinous ligament is a continuation of ligamentum nuchae, an elastin-based ligament that runs from the base of the skull to the midthoracic spinous processes. As it extends caudally, it becomes a very stiff collagenous band that connects the spinous processes of the lower thoracic and lumbar vertebrae. The absence of this stiff connection across the lumbosacral joint could allow greater joint mobility. The lumbosacral joint is intimately associated with the propulsive apparatus, notably the hind limbs and pelvic girdle. Large terrestrial quadrupeds possess substantial gluteal muscles. Part of the main gluteal mass, the gluteal tongue, often crosses the lumbosacral joint to insert onto the vertebral processes of the lumbar vertebrae (Slijper, 1946). The gluteal tongue of horses can be quite substantial, inserting as far forward as L1L2 (Jeffcott and Dalin, 1980; Townsend *et al.* 1983). Contraction of the gluteal musculature, including the gluteal

tongue, would cause hip and lumbosacral extension. Both of these anatomical features could potentially enhance the forced angular range of the lumbosacral joint. Exploring the energetic consequences of operating and controlling a spine with highly localized mobility, as opposed to one with more evenly distributed mobility, was beyond the scope of this study. It remains an interesting problem for future consideration.

Fig. 8 summarizes the relative sagittal bending behaviour of these mammals. Despite having similar forced bending ranges, monkey joints were much more resistant to bending than those of rabbits, badgers and wallabies. In fact, relative to their size, the monkey spines were the most resistant of this diverse sample. The seal joints were unique for their relatively large bending ranges and apparently low resistances in both extension and flexion. Neutral zones in seal lumbar–lumbar and lumbosacral joints were significant and substantial. Indeed, relative to those of sheep of similar mass, lumbar–lumbar bending resistance appeared very low (compare the open bars in the histograms of Fig. 8). There appears to be no clear geometric scaling effect in this small and taxonomically diverse sample of mammalian species. The rabbits and monkeys were of similar body mass and had comparable forced mobility ranges. However, the monkey joints appeared to have greater relative bending resistance. Elastic and static stress similarity theory, as applied to the bending vertebrae of this study, would require that the bending moments be divided by body mass raised to powers greater than one ( $5/4$  and  $7/5$  respectively). The reduction in specific bending moment would be relatively greater for the larger animals than for the smaller ones, but the disparity between the monkey and other species, for example, is not altered by the adoption of either elastic or static stress similarity (calculated but not shown here). Neither does there appear to be any obvious relationship between the relative epaxial and hypaxial muscle masses (Table 1) and the static bending characteristics of the lumbosacral spines tested here. Slijper (1946) suggested that spinal muscle architecture was dictated to a large extent by the locomotor demands of the animal. It would appear that locomotor and behavioural characteristics have an effect on the functional morphology of the vertebral axial skeleton.

The static bending tests proved to be useful for exploring relative bending behaviour and end-point bending properties. However, intervertebral joints are subject to dynamic as well as static loading regimes. Because of the relatively low sensitivity of the static bending frame, it was very difficult to measure accurately angular deformations at low specific bending moments. Performing dynamic bending tests with more sensitive apparatus allowed one to draw conclusions about joint behaviour under more physiological loading regimes. Although absolute moments may be considerable, fine dynamic adjustments in the balance of moments about joints probably have important consequences for controlling posture and locomotor curvatures.

Dynamic bending tests were performed with joint complexes derived from additional monkey, wallaby and tiger spines. These species were selected because all of them displayed flexion asymmetry in their respective forced bending ranges. They also exhibited limited extension ranges. Conducting dynamic tests with seal joint complexes allowed a unique opportunity to compare and contrast detailed information about the sagittal bending behaviour of terrestrial with semi-aquatic mammals. It was hoped that

the dynamic bending experiments would shed more light on relative bending stiffnesses, properties that would require measurements of low moment deformation. It would appear that the aforementioned goals have been met with some success. However, any conclusions drawn from the results of the dynamic bending experiments depend upon the extent to which the model parameters  $A$ ,  $B$ ,  $C$  and  $D$  really reflect differences in the physical properties of the bending intervertebral joints.

The model used for bending was  $y=A(1-e^{-Bx})$ , a simple, asymptotic function with a non-zero slope when  $x$  equals zero. It reflected the physical observation that intervertebral joint angle would increase with increasing bending moment up to a certain level, beyond which further deformation would ultimately lead to joint failure.  $A$  is the asymptote of the function. It therefore represents a joint's capacity for angular change.  $B$  is the constant that indicates the rate at which the asymptote is achieved. It is indicative of a joint's compliance in bending. The greater the  $B$  value, the lower the bending resistance or stiffness of the joint.

A protractor was used to measure intervertebral angles from tracings of the X-radiographs. The measurement error associated with this technique was  $\pm 1.0^\circ$ . Therefore, the relative measurement errors of small intervertebral angles were greater than those for large angles. Estimates of  $B$  required information about angles and bending moments on the approach to the asymptotic plateaus. Because the extension asymptotes were often quite small ( $+3$  to  $+8^\circ$ , see Tables 2–4), the scatter of the data, and hence the standard errors of the extension  $B$  values, was often considerable. Indeed, if low-moment data were lacking and the plateaus appeared to materialize almost immediately, the non-linear iterative procedures used to determine the model parameters gave virtually infinite slopes (i.e. very large  $B$  values) with undefined standard errors (equal to zero) (e.g. wallaby L5L6 in extension,  $B=1249.7$ , and monkey L3L4 in extension,  $B=4.7 \times 10^{10}$ , for example, see Tables 3 and 2 respectively). This partly contributed to the acceptance of the null hypothesis for comparisons of homologous extension functions in the midlumbar joints of the land animals.

Clear outlines were required to estimate the orientation of the central long axes of the vertebrae. This was difficult for the central vertebrae of the smaller specimens because they were often partly obscured by the width of the steel clamp. In these situations, the angles of the intervertebral joints were measured with respect to the parallel sides of the steel clamp. This was legitimate since the goal was to measure changes in intervertebral angles. However, this method assumed that there was no rotation of the central vertebrae with respect to the clamp. In specimens where the central vertebrae were clearly visible, the angles between the parallel sides of the clamp and the long axes of the central vertebrae were measured. These angles remained constant for all X-rays within any bending test. Rotation of central vertebrae with respect to the clamp did not occur during these tests to any measurable degree. This was partly because efforts were made to apply symmetrical bending moments to the intervertebral joints by positioning the metal blocks equidistant from the disc centres. Additionally, the results of the static bending experiments suggested that adjacent lumbar–lumbar joints had similar bending properties, so symmetrical bending about the central vertebrae was a valid assumption for lumbar–lumbar specimens. Specimens involving the lumbosacral joints were less of a

problem because low lumbar and lumbosacral vertebrae were sufficiently large for the angles of the vertebral centra to be measured directly.

Despite the minimum ten-cycle conditioning of each specimen, a slight decrease in force was sometimes observed while the machine was stopped in mid-cycle to expose an X-ray plate. Since these decreases in force were less than 5% of the initial maxima, they were considered to be negligible.

These experiments involved applying forces about moment arms limited by the dimensions of the vertebrae. For some specimens, particularly those from the monkeys and smaller wallabies, the required forces were relatively large compared to the stiffness of the threaded steel bar transmitting the specimen force to the load cell. Since the specimen, threaded bar and clamp were in series, the forces measured by the load cell were those applied to the intervertebral joints. However, the work done by the Instron included the work done to bend the joints and the threaded steel bar. The strain energies absorbed by the steel bars were subtracted from the total strain energies recorded. The remainder was shared between the two joints, depending upon the changes in intervertebral angle observed. Joint resilience was estimated by quantifying the energy released by the specimens as they were allowed to return to their original states. In these calculations, it was assumed that the resilience of the threaded steel bars was 100%. This was certainly the case for the short-term compliance tests. However, after the bending experiments had been completed and the threaded bars were removed from the specimens, very slight distortions were sometimes observed in the centre of the bars. This meant that some of the work done to deform the bars was not recovered and that the resiliences of the bars were less than 100%. Therefore, the intervertebral joint resiliences quoted in Table 8 may have been slightly underestimated.

Fig. 8 shows the bending responses of intervertebral joints from the seven initial species to specific static bending moments. It gives the impression that the lumbosacral joints of some species are much less resistant to bending than are the adjacent lumbar–lumbar joints (wallaby and tiger, for example). However, the maximum ratios for the static bending comparisons ( $\pm 0.10 \text{ Nm kg}^{-1}$ ) were chosen because they were within the ranges of applied moments of nearly all of the experimental data sets, so that extrapolations were avoided. If a particular moment ratio forced a plateau angle in one joint but not in an adjacent joint, the latter would appear less resistant to the bending mode concerned. The results of the dynamic bending experiments (see Tables 2–5) show that the compliances ( $B$  values, indices of joint stiffness) of the lumbar–lumbar and lumbosacral joints are similar within the species groups selected. Lumbosacral joints differed from lumbar–lumbar joints primarily in their enhanced capacities for bending.

This may not be the case for all mammalian lumbosacral joints. As discussed previously, the lumbosacral joints of some species seem to be anatomically predisposed to large ranges of movement. The lumbosacral articulations themselves are uniquely constructed in horses and rhinoceroses, for example. The transverse processes of the most caudal lumbar vertebrae form synovial articulations with the sacral wings. This hinge-like effect is enhanced by the fusion of some of the lower lumbar transverse processes, thus further restricting lumbar movement to the lumbosacral articulation. Synovial joints have characteristically low friction, so it is possible that the lumbosacral joints of horses

and rhinoceroses have different resistances to bending compared to their lumbar–lumbar counterparts, in addition to their enhanced capacities for bending (Jeffcott and Dalin, 1980; Townsend and Leach, 1984).

Comparisons of homologous terrestrial mid-lumbar joints in extension show insufficient differences to warrant separate functions (see Table 7). As stated earlier, comparisons were confounded by the relatively large standard errors of their  $B$  values (see Tables 2–4). Extension capacities were typically limited to about  $3\text{--}8^\circ$ . However, the extension compliances and plateaus were much greater in the seal joints. It may be reasonable to assume that *in vivo* spinal extension (positive bending or sagging) is at least partly a gravitational phenomenon. Beam sagging, for example, may be induced by the support of a suspended weight. One might expect that the extension properties of intervertebral joints should follow a scaling law if the quadrupedal spine behaves like a horizontal beam supporting the abdominal mass. Elastic similarity theory (McMahon, 1973; 1975) states that structural dimensions should scale such that gravity-induced buckling is avoided. Here, bending moments have been divided by body mass. It is not obvious that dividing the bending moments applied by body masses raised to exponents greater than one (see Materials and methods, *The static bending experiments* for details) would alter the standard errors of the extension parameters of the joints of terrestrial species and clarify statistical similarities and differences. Perhaps the absence of the constant pull of gravity has somehow lessened the requirement for a very stiff spine in the semi-aquatic seal.

Homologous joint comparisons in flexion (see Fig. 10B for example) showed four compliances for the four groups. High-flexion compliances in the seal joints were similar to the high-extension compliances. However, monkey and wallaby flexion compliances ( $B$  values) were considerably less than those for the tiger and jaguar joints. Interestingly, monkey and wallaby flexion capacities ( $A$  values) were greater than those for the tiger and jaguar joints. Therefore, despite having relatively higher flexion stiffnesses, monkey and wallaby joints had greater flexion capacities than homologous tiger and jaguar joints. It remains to be seen what structures are responsible for endowing these species with the observed bending properties.

Specific strain energy functions for intervertebral joints of the different species in extension and flexion appeared to be sufficiently different to warrant description by separate functions ( $Q$  test results, Table 8). Much less work was required to bend the seal joints than to bend the joints of the land mammals. More specific energy was required to extend and flex the monkey joints than to bend the tiger and jaguar joints. Exponents of the power curves were generally less than 2, that expected for a Hookean spring. However, given the magnitudes of the standard errors, these exponents are probably not different from 2. Most biological materials show non-linear elastic behaviour (Wainwright *et al.* 1976) so that one might have expected exponents even greater than 2. This was observed only in the tiger/jaguar flexion results.

Approximate intervertebral joint resiliences are listed in Table 8. Although terrestrial joint resiliences were similar in extension, tiger/jaguar flexion resilience was much less than those for monkey and wallaby joints. Joint resiliences may have been underestimated if the resiliences of the steel bars were overestimated. There was evidence

of the latter (slight irreversible distortions of the bar) following some of the bending tests of all except the seal specimens. From these experiments, it is not clear why tiger and jaguar resiliences were so low.

The results of these experiments suggest that bending resistance, particularly to flexion moments, may be manifest by different materials and/or structures in monkeys, wallabies, tigers and jaguars and seals. All of the terrestrial species showed similar tendencies towards enhanced joint flexion, relative to extension. However, the compliances differed markedly. Monkey and wallaby joints were relatively stiffer in flexion than tiger/jaguar joints, despite having greater flexion ranges. Most discussions of mammalian intervertebral joint mobility and/or flexibility make no distinction between these two aspects of joint movement (Jeffcott and Dalin, 1980; Townsend *et al.* 1983; Halpert *et al.* 1987, for example). Perhaps hypotheses pertaining to stiff and/or flexible spinal morphologies (Smeathers, 1981, for example) require reconsideration.

The author gratefully acknowledges the financial support of an NSERC PGS4 scholarship and ORS and Tetley-Lupton awards. Special thanks are due to Professor R. McNeill Alexander for his helpful advice on this work. Dr Caroline Pond provided assistance in the acquisition of many of the experimental specimens.

### References

- ALEXANDER, R. MCN. (1988). Why mammals gallop. *Am. Zool.* **28**, 237–245.
- ALEXANDER, R. MCN., DIMERY, N. J. AND KER, R. F. (1985). Elastic structures in the back and their role in galloping mammals. *J. Zool., Lond.* **A 207**, 467–482.
- BADOUX, D. M. (1968). Some notes on the curvature of the vertebral column of vertebrates with special reference to mammals. *Acta morph. neerl.-scand.* **1**, 29–40.
- BMDP (1988). *Biomedical Computer Programs*. 1988 edition. University of California Press, 2223 Fulton Street, Berkeley, California, 94720.
- BURN, D. M. (1980). *The Complete Encyclopaedia of the Animal World*. London: Octopus Books Ltd.
- BURTON, M. (1972). *Encyclopaedia of Animals*. London: Octopus Books Ltd.
- BURTON, M. AND BURTON, R. (1979). *Encyclopaedia of Mammals*. London: Galley Press, Cathay Books.
- DILLON AND GOLDSTEIN (1984). *Multivariate Analysis – Methods and Applications*. New York: Wiley.
- EDWARDS, W. T., HAYES, W. C., POSNER, I., WHITE, A. A. AND MANN, R. W. (1987). Variation of lumbar spine stiffness with load. *J. biomech. Eng.* **109**, 35–42.
- GETTY, R. (1975). *Sisson's and Grossman's Anatomy of the Domestic Animals*. Fifth edition. Philadelphia: Saunders.
- HALPERT, A. P., JENKINS, F. A. AND FRANKS, H. (1987). Structure and scaling of the lumbar vertebrae in African bovids (Mammalia: Artiodactyla). *J. Zool., Lond.* **211**, 239–258.
- HANSSON, T. H., KELLER, T. S. AND PANJABI, M. M. (1986). A study of the compressive properties of lumbar vertebral trabeculae: Effects of tissue characteristics. *Spine* **12**, 56–62.
- HILDEBRAND, M. (1959). Motions of the running cheetah and horse. *J. Mammal.* **40**, 481–495.
- HUROV, J. R. (1987). Terrestrial locomotion and back anatomy in vervet (*Circopithecus aethiops*) and patas (*Erythrocebus patas*) monkeys. *Am. J. Primatol.* **13**, 297–311.
- JAYSON, M. I. V. (1980). Structure and function of the human spine. In *Engineering Aspects of the Spine*. The Institution of Mechanical Engineers, London: Mechanical Engineering Publications Ltd. pp. 41–42.
- JEFFCOTT, L. B. AND DALIN, G. (1980). Natural rigidity of the horse's backbone. *Eq. vet. J.* **12**, 101–108.
- KIM, Y. E. AND GOEL, V. K. (1990). Effects of testing mode on the biomechanical response of a spinal motion segment. *J. Biomech.* **25**, 289–291.
- MCMAHON, T. (1973). Size and shape in biology. *Science* **179**, 1201–1204.

- McMAHON, T. (1975). Using body size to understand the structural design of animals: quadrupedal locomotion. *J. appl. Physiol.* **39**, 619–627.
- MILLER, J. A. A., SCHULTZ, A. B., WARWICK, D. N. AND SPENCER, D. L. (1986). Mechanical properties of lumbar spine motion segments under large loads. *J. Biomech.* **19**, 79–84.
- OSVALDER, A. L., NEUMANN, P., LOVSUND, P. AND NORDWALL, A. (1990). Ultimate strength of the lumbar spine in flexion – an *in vitro* study. *J. Biomech.* **23**, 453–460.
- ROCKWELL, H., EVANS, F. G. AND PHEASANT, H. C. (1938). The comparative morphology of the vertebrate spinal column: Its form as related to function. *J. Morph.* **63**, 87–117.
- ROHLF, F. J. AND SOKAL, R. R. (1981). *Statistical Tables*. Second edition. New York: W. H. Freeman and Company.
- SAS (1985). *SAS User's Guide: Statistics Version*. Fifth edition. Cary, NC, USA: SAS Institute Inc.
- SHIRAZI-ADL, A. AND DROUIN, G. (1987). Load-bearing role of facets in a lumbar segment under sagittal plane loadings. *J. Biomech.* **20**, 601–613.
- SLIJPER, E. J. (1946). Comparative biologic–anatomical investigations on the vertebral column and spinal musculature of mammals. *Verh. Kon. Nederl. Akad. Wetensch. Amsterdam II* **42**, 1–128.
- SMEATHERS, J. E. (1981). *A Mechanical Analysis of the Mammalian Lumbar Spine*. PhD thesis, Department of Zoology, University of Reading, UK.
- SMEATHERS, J. E. AND JOANES, D. N. (1988). Dynamic compressive properties of human lumbar intervertebral joints: A comparison between fresh and thawed specimens. *J. Biomech.* **21**, 425–433.
- SOKAL, R. R. AND ROHLF, F. J. (1981). *Biometry*. Second edition. New York: W. H. Freeman and Company.
- THOMPSON D'A, W. (1917). *On Growth and Form*. Cambridge: Cambridge University Press.
- TIMOSHENKO, S. AND MACCULLOUGH, G. H. (1948). *Elements of Strength of Materials*. New York: D. Van Nostrand Company, Inc.
- TOWNSEND, H. G. G. AND LEACH, D. H. (1984). Relationship between intervertebral joint morphology and mobility in the equine thoracolumbar spine. *Eq. vet. J.* **16**, 461–465.
- TOWNSEND, H. G. G., LEACH, D. H. AND FRETZ, P. B. (1983). Kinematics of the equine thoracolumbar spine. *Eq. vet. J.* **15**, 117–122.
- WAINWRIGHT, S. A., BIGGS, W. D., CURREY, J. D. AND GOSLINE, J. M. (1976). *Mechanical Design in Organisms*. Princeton, New Jersey: Princeton University Press.
- WHITE, A. A. AND PANJABI, M. M. (1990). *Clinical Biomechanics of the Spine*. Philadelphia, Pennsylvania: J. B. Lippincott Company.
- YAMAMOTO, I., PANJABI, M. M., CRISCO, T. AND OXLAND, T. (1989). Three dimensional movements of the whole lumbar spine and lumbosacral joint. *Spine* **14**, 1256–1260.
- YOGANANDAN, N., RAY, E., PINTAR, F. A., MYKLEBUST, J. B. AND SANCES, A. (1989). Stiffness and strain energy criteria to evaluate the threshold of injury to an intervertebral joint. *J. Biomech.* **22**, 135–142.